Density-matrix renormalization-group study of low-lying excitations of polyacene within a Pariser-Parr-Pople model

C. Raghu,* Y. Anusooya Pati,† and S. Ramasesha‡
Solid State and Structural Chemistry Unit, Indian Institute of Science, Bangalore 560 012, India
(Received 27 December 2001; revised manuscript received 3 April 2002; published 29 July 2002)

We have carried out symmetrized density-matrix renormalization-group calculations to study the nature of excited states of long polyacene oligomers within a Pariser-Parr-Pople Hamiltonian. We have used the C_2 symmetry, the electron-hole symmetry, and the spin parity of the system in our calculations. We find that there is a crossover in the lowest dipole forbidden two-photon state and the lowest dipole allowed excited state with size of the oligomer. In the long system limit, the two-photon state lies below the lowest dipole allowed excited state. The triplet state lies well below the two-photon state and energetically does not correspond to its description as being made up of two triplets. These results are in agreement with the general trends in linear conjugated polymers. However, unlike in linear polyenes wherein the two-photon state is a localized excitation, we find that in polyacenes, the two-photon excitation is spread out over the system. We have doped the systems with a hole and an electron and have calculated the charge excitation gap. Using the charge gap and the optical gap, we estimate the binding energy of the 1^1B^- exciton to be 2.09 eV. We have also studied doubly doped polyacenes and find that the bipolaron in these systems, to be composed of two separated polarons, as indicated by the calculated charge-density profile and charge-charge correlation function. We have studied bond orders in various states in order to get an idea of the excited state geometry of the system. We find that the ground state, the triplet state, the dipole allowed state, and the polaron excitations correspond to lengthening of the rung bonds in the interior of the oligomer while the two-photon excitation corresponds to the rung bond lengths having two maxima in the system.

DOI: 10.1103/PhysRevB.66.035116 PACS number(s): 71.10.Fd, 71.30.+h, 71.45.−d, 31.25.Qm

I. INTRODUCTION

There has been a resurgence of interest in the conjugated polymer polyacene, since Batlogg and co-workers reported lasing in the first organic solid-state injection laser based on single crystals of tetracene.[1] They also obtained very high electron and hole mobilities at very low temperature—of the order of 10^4–10^5 $cm^2\,V^{-1}\,s^{-1}$—in metal-insulator-semiconductor (MIS) devices prepared from crystals of tetracene and pentacene.[2] A wide variety of exotic physical phenomena like fractional quantum Hall effect, superconductivity, metal-insulator transitions, and electrical switching behavior have been observed in the field effect transistor (FET) devices based on tetracene and pentacene.[3,4] These discoveries have revolutionized the field of organic molecular semiconductors and understanding the observed transport and optical phenomena theoretically presents a grand challenge. At the same time, these molecular materials have a strong limitation for application in optical communications. They emit in the visible or UV range of the spectrum, while active materials for optical communications need to emit in the infrared.[5] It is well known that polymers have smaller optical gaps than oligomers and hence our interest in large polyacene systems, $C_{4n+2}H_{2n+4}$. However, it must be mentioned that experimentally larger polyacenes are difficult to prepare in the laboratory and the largest oligomer reported so far, $C_{30}H_{18}$, has seven benzene rings.

Oligomers of polyacene have been studied for a long time both experimentally and theoretically; the electronic structure has especially been an object of long-standing theoretical interest. Structurally, polyacene can be thought of as two coupled chains of polyacetylene (PA). A unit cell of polyacene consists of four carbon atoms in the sp^2 hybridized state. The p_z orbital of these carbon atoms give rise to four π bands which are half filled. These bands are classified as symmetric and antisymmetric, according to the symmetry of the molecular orbitals with respect to reflection about the plane that bisects the chain.[6] Within the Hückel model, the energy gap is zero for symmetric polyacene. Longuet-Higgins and Salem considered the question of Peierls' distortion of the polymer in the extended limit. They argued that the system was not susceptible to the Peierls' distortion, due to an unusual feature of the band dispersion for polyacene, namely, the occurrence of a degeneracy between bands of opposite symmetry at the Fermi surface. The question of Peierls' instability in polyacenes using the Pariser-Parr-Pople model, which is an extended range interacting model, has been addressed by the present authors in a separate paper.[7] Several semiempirical methods, as well as complete active space perturbative methods, have been used for studying the low-lying states of polyacene.[8,9] Recently, Bredas *et al.* have used a semiempirical Hartree-Fock intermediate neglect of differential overlap (INDO) method to study the band gap of pentacene single crystal.[9] From the highest occupied molecular orbital/lowest unoccupied molecular orbital (HOMO-LUMO) levels of INDO calculation, they have obtained the band gap which is comparable with that of tetrathiofulvalene-tetracyanoquniodimethane (TTF-TCNQ), an organic charge-transfer salt.

In the case of conjugated polymers, it has been found that doping of the polymer makes them conducting. Conductivity as high as 10^5 S/cm has been observed in the case of doped polyacetylene.[10] Su, Schrieffer, and Heeger have introduced

a model (the SSH model) for studying nonlinear excitations such as polarons, bipolarons, and solitons.[11] Solitonic excitations are observed only for those systems with degenerate ground state. Baeriswyl and Maki have introduced a simple model to deal with two coupled chains.[12] Sabra *et al.* have studied distribution of polaron and bipolaron on polyacene as two coupled chains of transpolyacetylene within the SSH model.[13] Later Li and co-workers have studied polaronic excitations in polyacene based on the extended SSH-Hubbard model.[14] They have obtained the dimerized displacement which is very similar to that of polyacetylene.

The main drawback of these studies is the neglect of explicit electron-electron correlation, known to be crucial even for a qualitative understanding of the excitation spectrum of conjugated systems. For example, in polyenes, there exists an optically forbidden covalent excitation below the optical gap, which cannot be explained within a simple noninteracting model. Electron correlation lowers the energy of dipole forbidden covalent excitations while raising the energies of the dipole allowed ionic excitations. Indeed, the former become the spin excitations of a Heisenberg antiferromagnet in the limit of large correlations. One of the major issues in the case of finite polyenes and PA is the relative positions of the optically allowed ionic $1B_u^-$ state and the covalent two-photon $2A_g^+$ state. In the long chain limit, the correct ordering, i.e., the $2A_g^+$ state below the $1B_u^-$ state, can be obtained only by including electron-electron interaction effects, as demonstrated by Soos and Ramasesha[15]. This is verified by the observation of a two-photon state below the optical gap in long polyenes and the weak photoluminescence in *trans*-PA is attributed to the existence of this dipole forbidden state below the optical gap. Contrary to the prediction of the noninteracting models, the optical gap is mainly determined by the strength of the Coulomb interaction; the contribution of lattice dimerization to the optical gap is minor.[16,17] In the case of finite polyenes, the two-photon state has been proposed to be made of two triplets.[18] A natural question is ''is this also valid in quasi-one dimension?,'' in the case of polyacene which can be thought of as two coupled PA chains.

Because of the large size of polyacene, it is difficult to study it within *ab initio* quantum chemical methods. However, as has been demonstrated for a wide range of π-conjugated molecules and polymers involving sp^2 carbon backbone, the Pariser-Parr-Pople (PPP) model, which includes explicit long-range electron-electron interactions, provides a physically consistent and numerically accurate description of these systems.[19,20] The largest oligomer of polyacene that has been studied so far, employing the PPP model within a full configuration interaction (CI) approach, is anthracene.[21] Larger oligomers of polyacene are, at present, not amenable to full CI studies.

Our aim here is to study large oligomers of polyacene systems within the PPP model.[19] The density-matrix-renormalization-group method (DMRG) has proved to be the best choice for studying one-dimensional as well as quasi-one-dimensional systems.[22] We have employed the symmetrized density-matrix-renormalization-group method (SDMRG), developed by Pati *et al.*,[23] to study the excited states of polyacene. To characterize these states, we have computed the properties such as bond order and charge and spin densities. In the next section we will describe briefly the computational method. The results and discussion will be given in the last section.

II. COMPUTATIONAL DETAILS

The PPP model has been widely studied in the context of conjugated polymers. The PPP Hamiltonian for polyacenes can be written as

$$\begin{aligned}\hat{H}_{\mathrm{PPP}} &= \sum_{l=1}^{2}\sum_{i,\sigma} t(\hat{a}^{\dagger}_{i,l\sigma}\hat{a}_{i+1,l\sigma} + \mathrm{H.\,c.}) \\ &+ \sum_{i,\sigma} t(\hat{a}^{\dagger}_{2i-1,1\sigma}\hat{a}_{2i-1,2\sigma} + \mathrm{H.\,c.}) \\ &+ \frac{U}{2}\sum_{i}\sum_{l}\hat{n}_{i,l}(\hat{n}_{i,l}-1) \\ &+ \sum_{i,j}\sum_{l,m} V_{il,jm}(\hat{n}_{i,l}-1)(\hat{n}_{j,m}-1), \end{aligned} \tag{1}$$

where l,m are the chain index, i,j refer to sites on a chain, $\hat{a}^{\dagger}_{i,l\sigma}(\hat{a}_{i,l\sigma})$ creates (annihilates) an electron of spin σ at site i on chain l, t is the transfer integral, U is the on-site Hubbard interaction, and $V_{il,jm}$ is the intersite Coulomb interaction. $V_{il,jm}$ is calculated based on the Ohno interpolation scheme,[24] widely used for conjugated polymers and given by

$$V_{il,jm} = 14.397\left[\frac{28.794}{(U_{il}+U_{jm})^2} + r^2_{il,jm}\right]^{-1/2}, \tag{2}$$

where the distance is in Å and the energies in eV. For all our calculations, we have used standard values for all parameters, namely $U = 11.26$ eV and $t = 2.4$ eV. The carbon-carbon bond length has been fixed at 1.397 Å and taken to be uniform for all the bonds.

We have used the symmetries C_2, electron hole, and spin parity which the polyacene chain possess. The chain has C_2 symmetry about the axis perpendicular to the plane containing the molecule. All carbon atoms on the chain are assumed to be equivalent, leading to the realization of alternancy symmetry or electron-hole symmetry for the system. The PPP Hamiltonian also conserves total spin S_{tot} and its z component S^z_{tot}. Here, we have only used spin parity which partitions the Hilbert space of the system into even and odd parity total spin sectors. The implementation of these symmetries in a DMRG procedure is discussed in detail in Ref. 23. The ground state of conjugated polymers usually lies in the even parity (e), ''covalent'' $(+)$ **A** subspace, denoted by ${}^e\mathbf{A}^+$. The optically allowed (dipole allowed) states lie in the even parity ''ionic'' ${}^e\mathbf{B}^-$ subspace. The optically forbidden two-photon state is the second singlet state in the covalent ${}^e\mathbf{A}^+$ subspace. The triplet states lie in the odd parity (o) subspace.

We start constructing the oligomers of polyacene from an initial system size of four sites. The systematic building up of various polyacene oligomers by adding two sites at a time in the DMRG iterations is illustrated in Fig. 1. This method of building the oligomers is found to be very accurate, from comparisons with results for the noninteracting systems

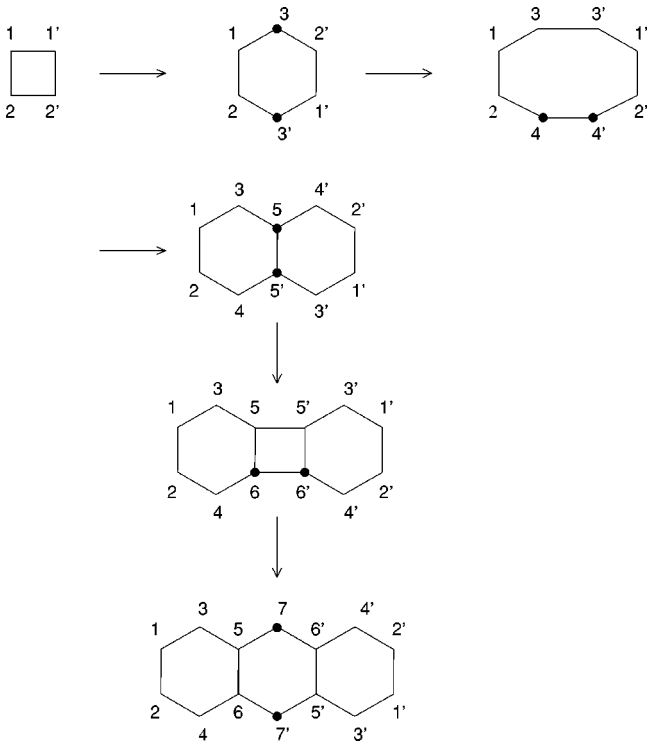

FIG. 1. Inside-out scheme for building polyacene oligomers. Two sites are added in the interior of the system at each iteration of the DMRG procedure, starting from a four site system. The primed sites correspond to the right block and the unprimed sites correspond to the left block.

which can be readily obtained. It is convenient to number the sites corresponding to left block (denoted by unprimed numbers) and right block (denoted by primed numbers) in such a way that at every stage of the DMRG procedure the primed and the corresponding unprimed sites belong to different sublattices of the bipartite polyacene system. This is achieved by rotating the right block by 180° about the molecular axis for system sizes corresponding to $4n$, n an integer.

To compute properties like densities and correlation functions, we have used the finite DMRG algorithm.[25] We have retained between 128 and 150 density-matrix eigenvectors in our calculations. We have incorporated long-range Coulomb interactions in our calculations. This involves storing and updating number operators for every site of the system at each DMRG iteration. Our scheme of numbering the bonds and sites for the largest system size attained is illustrated in Fig. 2. The rung bonds and leg bonds have been numbered separately, for convenience while discussing bond order results.

To establish the accuracy of our DMRG procedure, we have compared DMRG results for small system sizes, typically up to three rings with results obtained from exact diagonalization calculations in both the noninteracting limit of the Hamiltonian in Eq. (1) and with full interactions. To compare our results for the noninteracting Hamiltonian, we have done Hückel calculation up to a system size of ten rings. In Fig. 3, we have plotted the optical gap for the exact and DMRG calculations. We find that even in the noninteracting case where the DMRG accuracy is generally poor, the DMRG optical gaps compare favorably with exact results.

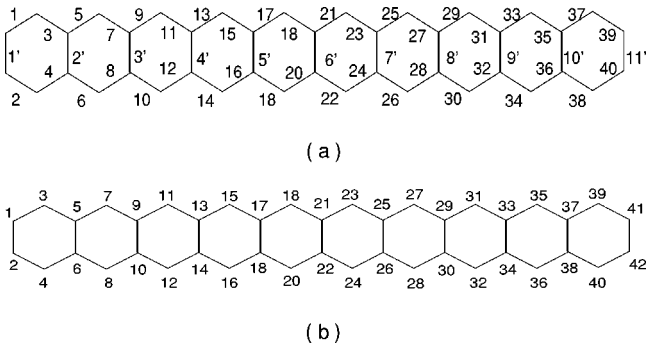

FIG. 2. Numbering scheme for (a) bonds and (b) sites in the ten-ring oligomer of polyacene. In (a), the rung bonds are numbered differently, with a prime.

For the interacting model, we have compared the DMRG results with exact diagonalization results obtained from the diagrammatic valence bond method[26] for system sizes of up to three rings. In Table I, we present this comparison for the energies of the ground state, the dipole allowed state, and the two-photon state of naphthalene and anthracene. The DMRG numbers are obtained from infinite DMRG algorithm with a cutoff m of 128 states. As can be seen from the table, we get very accurate energies for all these three states. This also establishes that we have successfully treated long-range Coulomb interactions in our DMRG calculations. In Table II we give the ground-state energy with three different DMRG cutoffs m for system sizes with up to five rings, within the finite DMRG algorithm with three finite DMRG iterations. We find that the change in ground-state energy on increasing m from

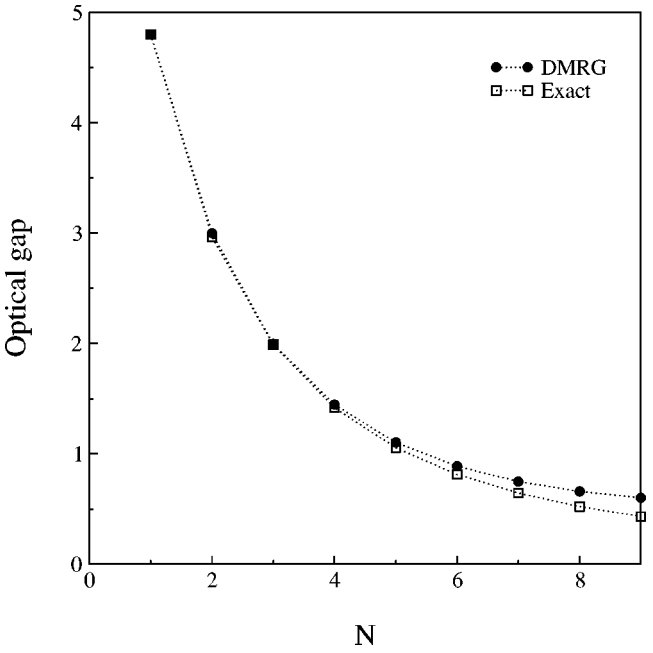

FIG. 3. Comparison of the optical gap (in eV) from exact Hückel calculation with those obtained from DMRG calculations for polyacenes with N rings.

TABLE I. Comparison of DMRG energies with exact energies for ground state, dipole allowed state, and two-photon states of 10 (naphthalene) and 14 (anthracene) site oligomers of polyacenes within the PPP model.

No. of sites	State symbol	Exact energy	DMRG energy
10	$1A^+$	−24.026	−24.017
	$1B^-$	−19.562	−19.558
	$2A^+$	−19.145	−19.132
14	$1A^+$	−33.889	−33.807
	$1B^-$	−30.213	−30.127
	$2A^+$	−30.012	−29.818

150 to 200 is 0.007%. We retain $m=150$ in all our calculations, except for the study of bipolarons where we have retained $m=200$ states. Properties like bond orders, charge and spin densities, and charge- and spin-correlation functions have been compared, again with values obtained from exact calculations and they compare well.

III. RESULTS AND DISCUSSION

Our study of polyacene oligomers is divided into two parts. The first part deals with energetics of the excitations of the neutral and doped systems and the second part deals with the properties of these excited states. We have studied a system consisting of ten rings, calculated various energy gaps, expectation values, and correlation functions. The size of the system considered is sufficient to saturate most excitation gaps (except the two-photon gap), so that properties can be evaluated without danger of significant finite-size effects. The aim of this study is to examine the nature of the ground state and various excited states for a larger number of rings, and to obtain the values of gaps in the thermodynamic limit ($N\rightarrow\infty$) by extrapolation. This study also involves singly and doubly doped polyacene systems.

A. Excitation spectra of neutral and doped polyacene

In Fig. 4 we plot the energy per monomer against the inverse of the number of monomers for the ground state, and the one- and two-electron doped states, to demonstrate that our infinite DMRG calculations converge well with increasing system size. All three energies converge to the same value since the quantity plotted is energy per unit cell which is an intensive variable. The differences in energy per unit cell among the three cases vanish in the thermodynamic limit (number of unit cells $\rightarrow\infty$) since the difference in total energy at any given size between neutral and doped species is finite.

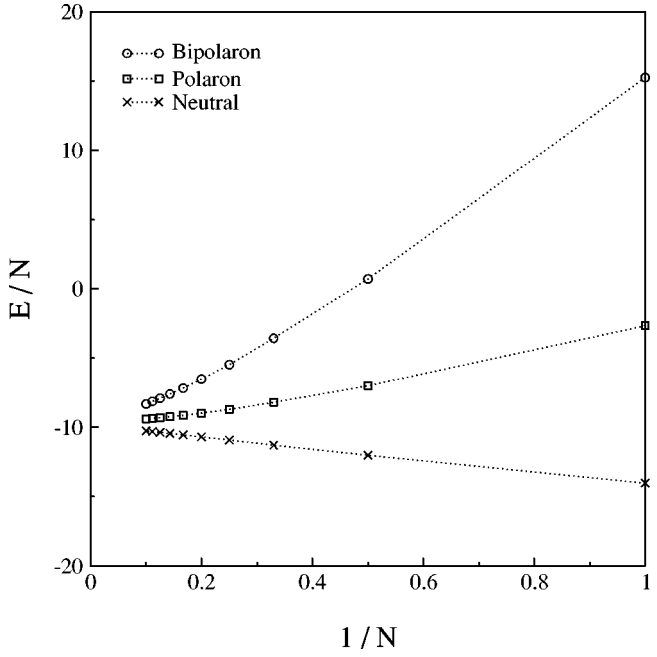

FIG. 4. Energy per monomer unit (in eV) for neutral, singly, and doubly electron doped polyacene as a function of inverse of the number of rings in the oligomer.

We have calculated the gaps from the ground state to various states of interest, like the one-photon state (1^1B^-) which is the lowest energy state in the $^{e}\mathbf{B}^-$ space, the two-photon state (2^1A^+) which is the second lowest energy state in the $^{e}\mathbf{A}^+$, and the lowest triplet state (1^3B^+), the lowest energy state in the space $^{o}\mathbf{B}^+$ space, for up to ten rings. In order to rule out the possibility that the second state in the $^{e}\mathbf{A}^+$ space in our case is indeed a singlet and not a quintet state, we carried out unsymmetrized DMRG calculations in the $M_s=2$ subspace. The lowest state in this subspace has a spin $\geqslant 2$. In Table III, we present the energies of the lowest state in the $M_s=2$ subspace and the energy of the 2^eA^+ state from symmetrized DMRG calculations. The difference in energy between the 2^eA^+ state and the lowest $M_s=2$ is well outside the accuracy of the DMRG calculations carried out using a DMRG cutoff $m=200$ with three finite iterations. If the $M_s=2$ was indeed a quintet state then the energy of this state should have been equal to the energy of the lowest state in the $M_s=2$ subspace within the accuracy of the DMRG calculations.

TABLE II. Comparison of DMRG ground-state energies with different cutoff m of density-matrix eigenvectors.

No. of sites	100	150	200
10	−24.0249	−24.0258	−24.0259
14	−33.8819	−33.8872	−33.8883
18	−43.7083	−43.7191	−43.7212
22	−53.5314	−53.5483	−53.5520

TABLE III. Energy for two-photon state and quintet states obtained from finite DMRG calculations with $m=200$.

No. of sites	2^1A^+	1^5A^+
10	−19.143	−17.466
14	−29.903	−28.484
18	−40.318	−39.470
22	−50.909	−50.197

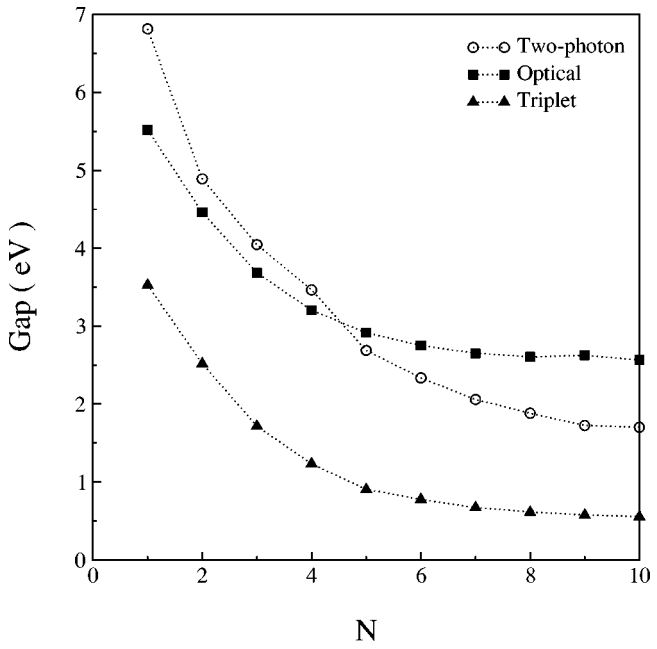

FIG. 5. Energy gaps in the PPP model to the lowest triplet state (filled triangles), dipole allowed one-photon state (squares), and two-photon state (circles) for polyacene plotted as a function of the number of rings in the system. Energy is given in units of eV.

In Fig. 5, we present the energy gaps as a function of the number of monomers. The small discrepancy in the optical gap for the nine ring polyacene reflects the magnitude of error in the computation of optical gaps. The DMRG optical gaps we have obtained for the eight, nine, and ten ring polyacenes are 2.60, 2.63, and 2.57 eV. For a smooth, monotonic decrease in the gap, the optical gap of the nine-ring polyacene should have been 2.59 eV, giving an approximate magnitude of the error in the optical gap of 0.04 eV. The gaps depend initially on the system size, but the optical and the spin gap saturate after about seven to eight monomer units. However, the two-photon gap does not saturate at this size. This suggests that the 1^1B^- and 1^3B^+ excitations are more localized than the two-photon excitation. This is quite unlike in polyenes where the two-photon state is more localized than the one-photon state.[27]

As is seen from the plot, the two-photon state initially lies above the lowest optically allowed state, but falls below the optical gap between a system size of four (tetracene) and five (pentacene) rings. From experiments, it is observed that the $1B_{2u}^-$ band (in our notation 1^1B^-) is redshifted by about 0.5–1.0 eV as the number of rings is increased from anthracene to pentacene. This shows that our results compare well with experiments. The $2^1A^+-1^1B^-$ crossover can be observed only in an interacting model[28] since in the noninteracting models this state is always above the one-photon state. This also points out that, according to Kasha's rule, naphthalene, anthracene, and tetracene should strongly fluoresce, which is indeed well known.

We can extrapolate the gaps in Fig. 5 to obtain their values in the polymer limit. The extrapolated values of the optical, two-photon, and spin gaps obtained are 2.46, 1.71, and 0.53 eV, respectively. Tavan and Schulten[18] had shown that the energy of the covalent excited state, $2A_g^+$, in polyenes is about twice that of the spin gap. What is interesting is the surprisingly low triplet gap in polyacenes, when compared to polyenes. This shows that the lowest two-photon state in polyacenes cannot be thought of as made up of two triplet excitations.

TABLE IV. Comparison of optical gap $=E(1^1B^-)-E(1^1A^+)$ and spin gap $=E(1^3B^+)-E(1^1A^+)$ from MRMP, DMRG, and experiment (values in eV), for various oligomers.

No. of rings	Nature of the gap	MRMP	DMRG	Experiment
3	Optical	3.40	3.68	3.31[a]
	spin	2.00	1.72	1.87[b]
4	Optical	2.80	3.20	3.43[c]
	spin	1.51	1.23	1.27[d]
5	Optical		2.92	2.28[e]
	spin		0.91	

[a]Reference 32.
[b]Reference 33.
[c]Reference 34.
[d]Reference 35.
[e]Reference 36.

We compare our calculations of the gaps with experimental values for some oligomers. Table IV gives the optical gap and spin gap for polyacenes from anthracene to pentacene from theoretical as well as experimental calculations. As is seen from the table, numbers obtained from the DMRG method are fairly close to experimental values in most cases, compared to the multireference Moller-Plesset perturbation (MRMP) calculations.[29] At this point, it is worth noting that the electron-hole symmetry in polyacenes is not a strict symmetry since all the carbon atoms in the system are not in an identical environment. Thus, in experiments, we should observe weak transitions between the ground state (which is in ''covalent'' **A** space) and states in covalent **B** space. This absorption will occur at a lower energy than the dipole allowed absorption since covalent states have lower energies than ionic states in correlated models. The optical gap presented in this paper corresponds to the transition from the ground state to the lowest energy state in ionic **B** space and hence will not strictly mark the absorption threshold in the UV visible spectrum.

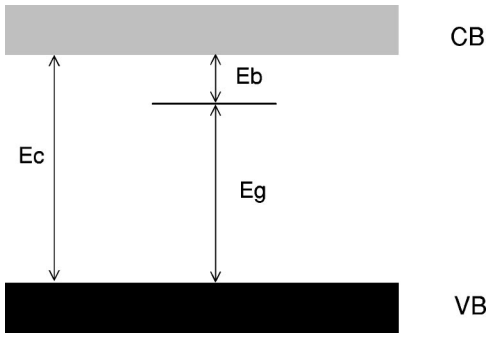

FIG. 6. Schematic description of formation of excitonic levels below the conduction band, showing a single excitonic level in the gap. E_c,E_g, and E_b are, respectively, the charge gap, the optical gap, and the exciton binding energy. VB and CB stand for the valence and conduction bands, respectively.

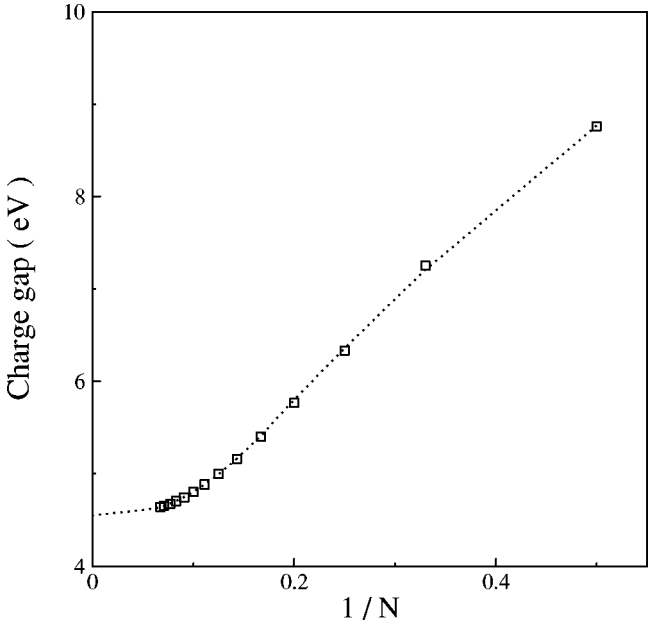

FIG. 7. The charge gap for polyacene (in eV), as a function of inverse system size. The dotted line through the data points is a guide to the eye used to obtain the extrapolated value of the charge gap.

We have considered various properties of doped polyacene like energy gaps, charge-density distribution, and bond orders, but these calculations have been performed ignoring the electron-lattice coupling on the basis that the time scales for these effects are much larger than the time scale for electronic excitations, and may be ignored in a first approximation (vertical ionization). Thus we are addressing only the vertical excitations and not the relaxed excitations in this study.

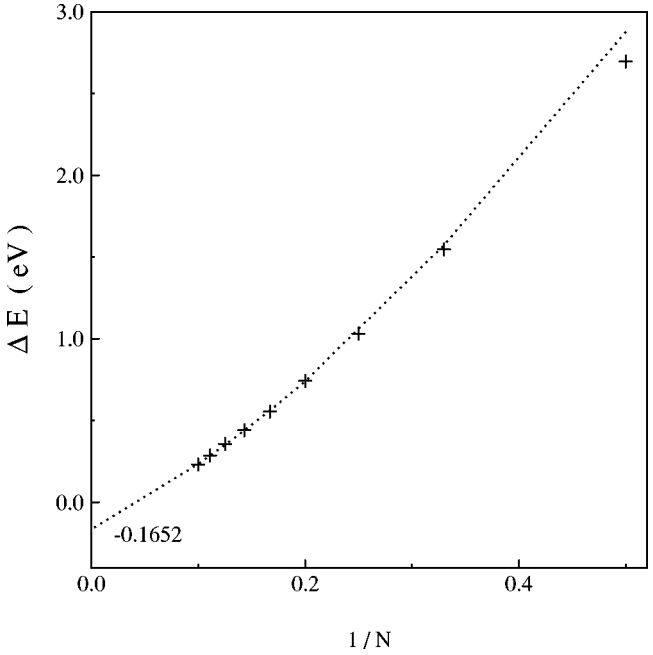

FIG. 8. The binding energy (in eV) of the bipolaron, as a function of inverse system size.

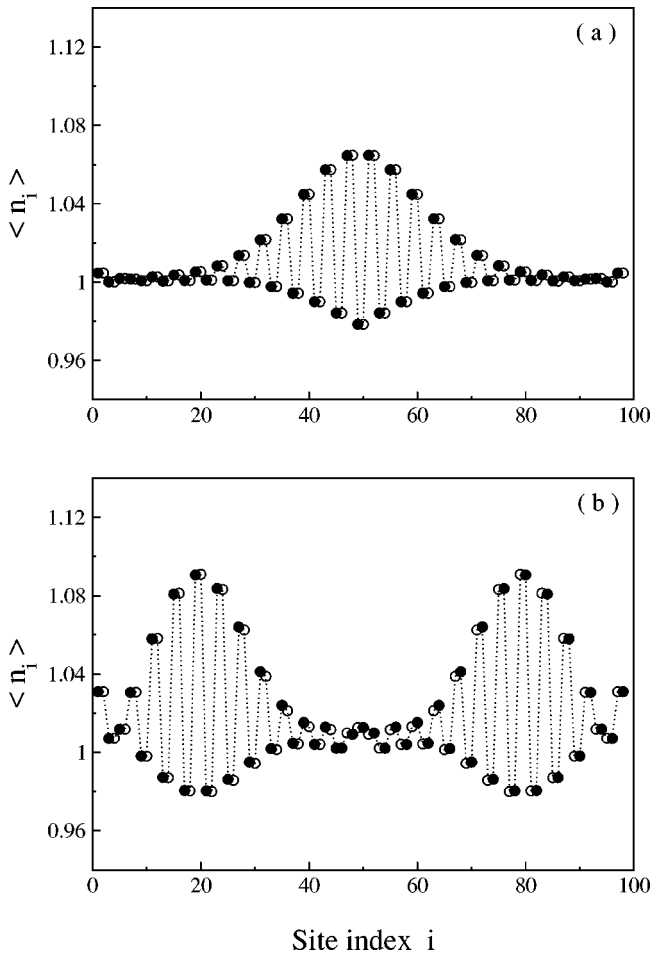

FIG. 9. Charge density for (a) polaron, and (b) bipolaron calculated for 24 monomer units. The filled circles represent the top leg and the empty circles the bottom leg of the polyacene ladder. The site numbering corresponds to Fig. 2.

The charge excitation gap in the Hückel model is the energy required to promote an electron from the top of the HOMO band to the bottom of the LUMO band. This process also corresponds to the photoexcitation threshold. Thus, in the Hückel model, the charge gap is the same as the optical gap for the system. In an interacting model, the charge excitation gap for a finite system is not necessarily the same as the photoexcitation threshold. If the only kind of electron-electron interaction considered in the model is the Hubbard on-site interaction, then the charge gap is the energy of an uncorrelated electron-hole pair, provided that all the transfer integrals are uniform. Once again the charge gap and the photoexcitation threshold coincide. If the range of the interaction extends beyond on-site, then the electron and the hole could form a bound state by residing in each other's vicinity leading to an exciton. Thus exciton formation takes place only in the UV or PPP models. In such a situation, the optical gap, i.e, the energy gap to the lowest dipole allowed state, is not same as the charge gap. The excitonic levels are formed close to the conduction-band edge, in a band picture, as shown in Fig. 6. The charge gap here is the sum of the optical gap and the exciton binding energy E_b. The exciton binding energy is the energy required to break up the bound

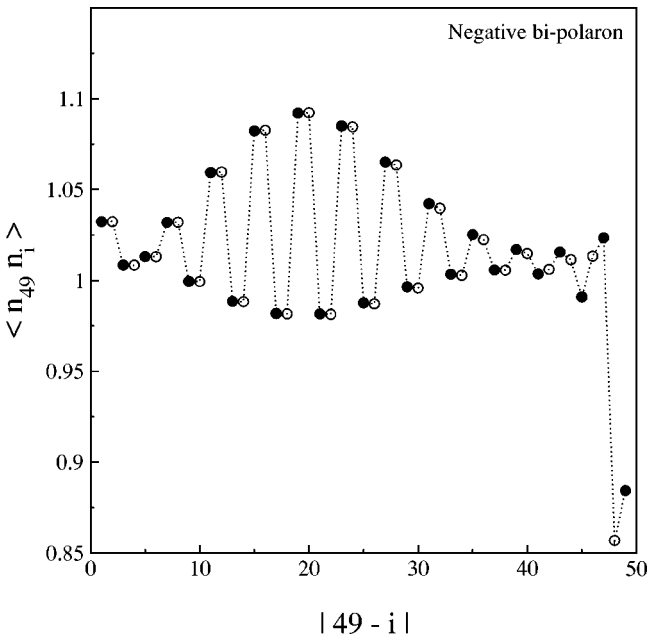

FIG. 10. Charge-charge correlation for the bipolaron, calculated for half of the polyacene chain with 24 rings. The filled circles represent the top leg and the empty circles the bottom leg of the polyacene ladder. The site numbering corresponds to Fig. 2.

electron-hole pair and promote them to the continuum, as represented by the conduction-band edge. To compute the charge gap, we consider the physical process which can be represented by the ''reaction''

$$2M \rightarrow P^+ + P^-, \tag{3}$$

where M is the neutral molecule and $P^{\pm}$ are the polarons. The energy for the above process can be computed by extrapolating to the thermodynamic limit $E_c(N)$ defined as

$$\begin{aligned} E_c(N) &= E_{P^-}(N) - E_M(N) + E_{P^+}(N) - E_M(N) \\ &= E_{P^-}(N) + E_{P^+}(N) - 2E_M(N), \end{aligned} \tag{4}$$

where $E_M(N)$ is the ground-state energy of the neutral oligomer, $E_{P^-}(N)$, that of negatively charged oligomer, and $E_{P^+}(N)$ of the positively charged oligomer, with the oligomer obtained from N monomers. In this real-space picture, the exciton binding energy may be calculated as $E_b = E_c(\infty) - E_g(\infty)$, where $E_g(\infty)$ is the extrapolated optical gap for the polymer limit.

We have calculated the charge gap for polyacenes with up to 15 rings. These are obtained from finite DMRG algorithm calculations in order to get as accurate values of the energy as possible. The charge gap result is displayed in Fig. 7, and the extrapolated value of the gap for $E_c(\infty)$ is obtained as 4.55 eV. From the value of the extrapolated optical gap which is 2.46 eV, we calculate the binding energy of the 1^1B^- exciton as 2.09 eV. This binding energy is larger than what has been estimated for polyenes or polypara pheneylene vinylenes.[30]

Overdoping the conjugated polymers can lead to removal (or addition) of two electrons, rather than one. These states

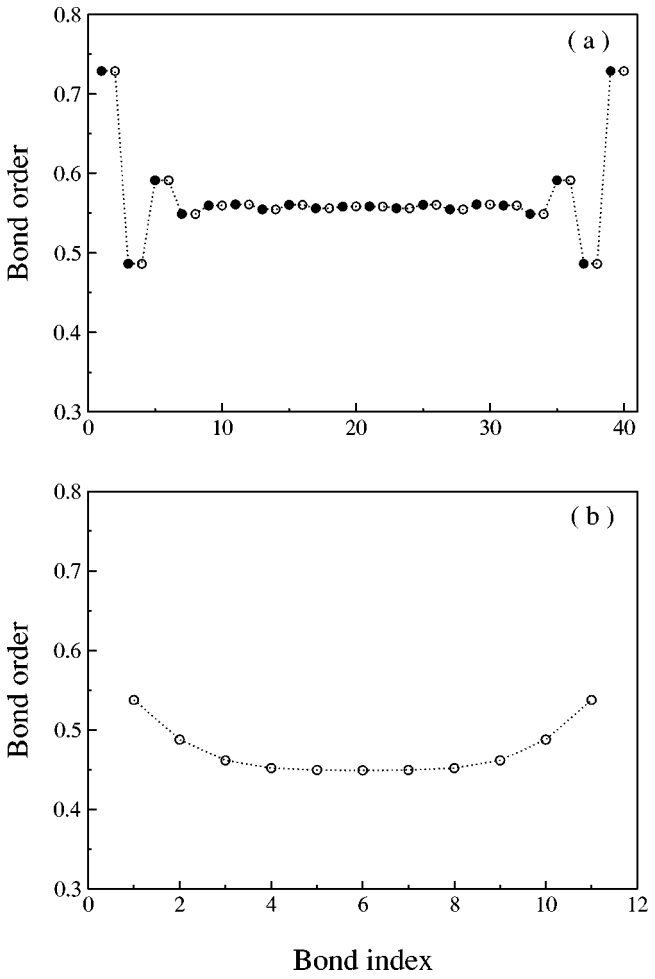

FIG. 11. Bond order in the ground state (1^1A^+) for polyacene, (a) for the legs of the ladder, (b) for the rungs. In (a), the filled circles represent the top leg and the empty circles the bottom leg of the ladder.

are termed positive (or negative) bipolarons. If we consider the formation of a bipolaron as a result of further removal (or addition) of an electron from a positive (or negative) polaron, then the question that comes up is ''is it energetically more favorable to remove (or add) a further electron from (to) a polaron or from anywhere else on the chain?'' In other words, we ask, is the bipolaron a stable entity or does it break up into two polarons? The process may be represented by the ''reaction''

$$P^+ + P^+ \rightarrow P^{++} + M. \tag{5}$$

If the energy change favors this process, then the bipolaron is likely to be a stable entity since the elastic energy in general favors the bipolaron formation. In a model such as the Hubbard model where the range of electron-electron interaction is severely truncated, the Coulombic effects will not favor a bipolaron formation. However, in the PPP model, the Coulomb interactions are long ranged and an explicit calculation is required to determine the possibility of bipolaron formation. We calculate the energy change for this process, $E_N(P^{++}) + E_N(M) - 2E_N(P^+)$ for finite oligomers of N

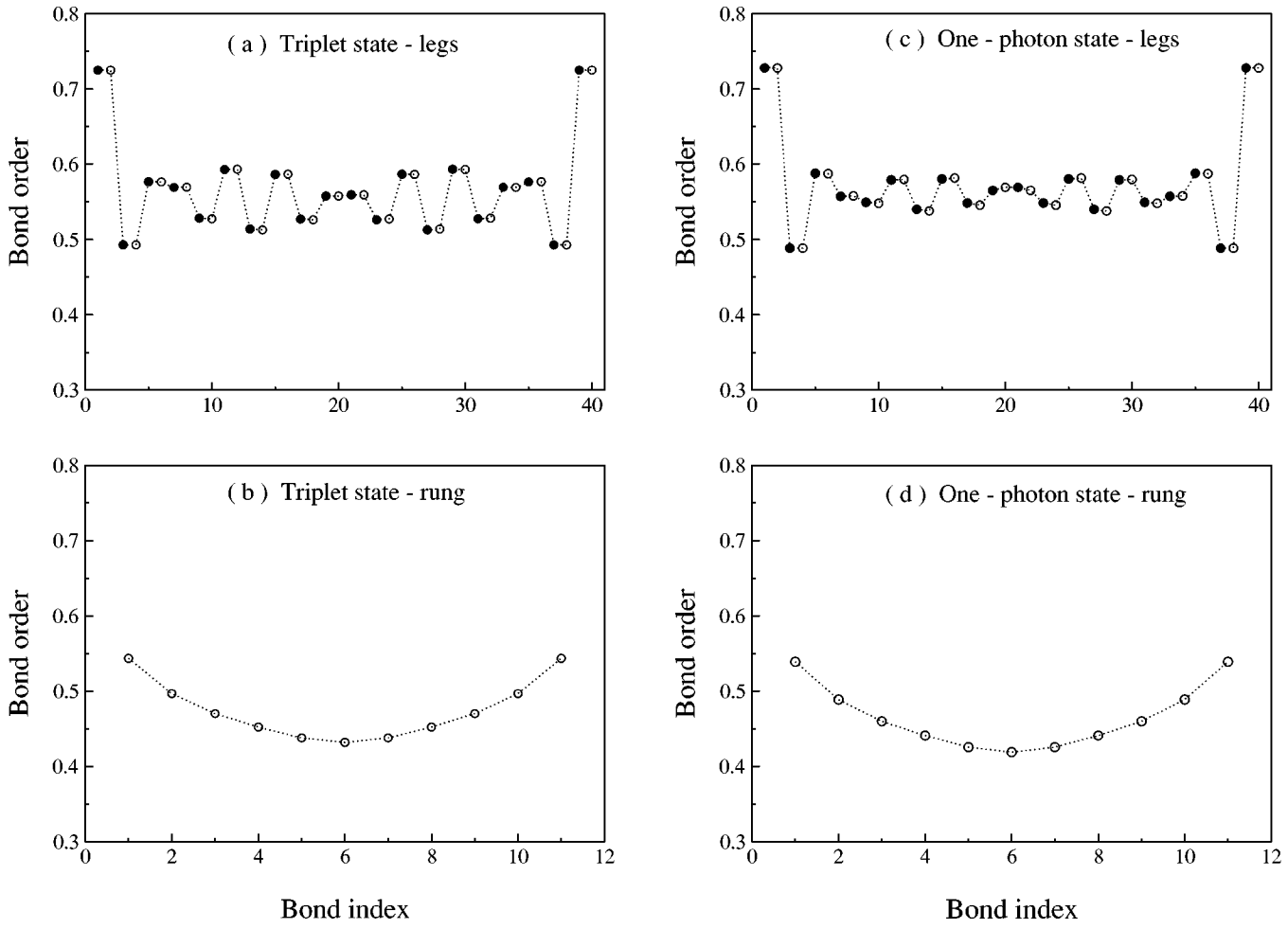

FIG. 12. Bond order in the 1^3B^+ and 1^1B^- states for polyacene, (a) for bonds on the legs, (b) for bonds on the rung for 1^3B^+ state, (c) for bonds on the legs, and (d) for bonds on the rung for 1^1B^- state. The empty circles represent the top leg and the filled circles the bottom leg of the ladder in (a) and (c). The numbering of the bonds corresponds to that described in Fig. 2.

units. If this difference is negative in the thermodynamic limit, then a bipolaron would be a stable entity upon formation. We have calculated the bipolaron stabilization energy as defined above an by infinite DMRG algorithm. We have used a higher DMRG cutoff of 200 density-matrix eigenvectors to get good convergence for the doubly doped systems. The result is displayed in Fig. 8. We obtain a small negative value of -0.163 eV for the binding energy. For the bipolaron to be stable, the binding energy has to be positive. The small negative number implies that the bipolaron is not a stable entity. However, because of the small magnitude of the binding energy and possible errors in extrapolation, we cannot definitely establish that the bipolaron is an unstable quasiparticle in these systems. For further verification of the nature of the bipolaron state, we have calculated the charge density for both polaron and bipolaron. These calculations are for a longer system size, i.e., 24 monomer units, as we wish to see the extent to which the excess charge is delocalized. The charge density for the singly doped state, displayed in Fig. 9(a), shows that the added excess charge is concentrated at the middle of the polyacene oligomer and it is spread over about 40 carbon sites, i.e., approximately ten rings. The charge density for the doubly doped state in Fig. 9(b) shows that the bipolaron is not a bound state, and disassociates into two polarons, which stay apart as much as possible to minimize Coulomb repulsion. The charge-charge correlation for the bipolaron in Fig. 10 confirms the above observations.

B. Bond orders for polyacene

A thorough investigation of the excited-state geometries either needs the computation of the equilibrium geometry to be obtained for each state independently or the computation of bond-bond correlation functions in the excited states and an analysis of the associated structure factors. However, bond orders computed for an excited state at the ground-state geometry can also throw some light on the equilibrium ge-

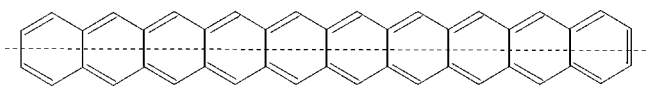

FIG. 13. ''Cis'' type of alternation of bonds in polyacene. The dotted line represents a plane of symmetry which bisects the molecule.

ometry the excited state may relax into. Indeed, Coulson's formula[31] assumes a direct relationship between bond length and bond order. Thus, for a π-conjugated chain, the bond orders in the ground state show an alternation even when the ground state is computed for a Hamiltonian with uniform bond lengths and associated transfer integrals, correctly implying that at equilibrium the chain will distort (Peierls' instability). Keeping this in view, we have investigated the geometry of the polyacene chain in the ground state and various excited states by calculating bond orders within these states obtained from the Hamiltonian at the ground-state geometry.

The bond orders have been calculated for the largest system size we have studied, i.e., for a polyacene with ten benzene rings. The bond order obtained in the ground state is shown in Fig. 11(a) for the leg bonds and in Fig. 11(b) for the rung bonds. Ignoring end effects the bond orders show that the bonds along the legs of the polyacene ladder are identical in length. The rung bond orders are smaller in magnitude, showing that they are longer than the leg bonds. Thus the ground state geometry of polyacene would correspond to two uniform polyene chains connected at alternate sites by a long bond.

The bond orders for the triplet 1^3B^+ state and the singlet 1^1B^- state are qualitatively similar, as seen in Figs. 12(a)–(d). The rung bond excitation is identical in both states, showing a lengthening of the rung bond towards the center of the chain, making it more ''single bond'' like in character. The bond orders on the legs of the ladder indicate an alternation of bond length along both legs of the polyacene ladder, towards the interior of the ladder.

Comparing both legs, we find that the alternation is of the ''cis'' type, as indicated in Fig. 13. This alternation looks more pronounced in the case of the triplet state than the 1^1B^- state. What is interesting to note is that the geometry in the ground state and in the excited states 1^1B^- and 1^3B^+ preserve the reflection symmetry about the plane containing the horizontal axis of the molecule, as indicated in Fig. 13 by the dotted line. This symmetry is not taken into account explicitly in our DMRG calculations, but is observed in the geometry of the above-mentioned states. The bond order in the singly electron doped system, the negative polaron, shown in Figs. 14(a) and (b), is qualitatively similar to that in 1^1B^- and 1^3B^+ states. Here, the rung bond distortion is comparable in magnitude to the other two states, but the leg bonds show a rather small alternation. The reflection symmetry of the molecule is preserved in this doped state as well.

The bond order in the two-photon state, displayed in Figs. 15(a) and (b) is much more complicated to analyze. This is consistent with the observation that the excitation is more delocalized than the other excitations discussed above. Indeed, to discern a pattern in the leg bonds, we need to study much larger oligomers. However, the rung bonds show a rather interesting and different pattern than the one observed for the one-photon and triplet excitations. The rung bonds in the two-photon state show a kink in the middle of the ladder, corresponding to a region in between where the bond lengths are shorter. In each half of the chain, the rung bond lengths go through a maximum. If we think of a single minima as in the triplet and one-photon state as corresponding to a standing half-wave in a box, then the two-photon state corresponds to a standing full wave in a box. The behavior of the rung bond order also shows why it is difficult to discern the pattern of the chain bond distortions in the two-photon state. It appears that two crossovers in bond alternation should be fitted within the chain length of the oligomer and 20 bonds in each chain of the ten-ring oligomer is too few to accommodate it. The bond order for rung and legs for the negatively charged bipolaron resembles the two-photon state bond orders, in Figs. 15(c) and (d). Here we clearly find a kink in the alternation pattern at the center of the chain. The alternation in the leg bonds is of a smaller magnitude compared to that of the two-photon state, as observed in the case of the negative polaron. The change in bond order values for the rung bonds is also of a smaller value compared to the two-photon state. In contrast to the 1^3B^+ and 1^1B^- states, 2^1A^+ breaks the symmetry of reflection about the horizontal plane in Fig. 13.

Tavan and Schulten have shown that the covalent excitation, $2^1A_g^+$, is accompanied by the change in bond order.[18]

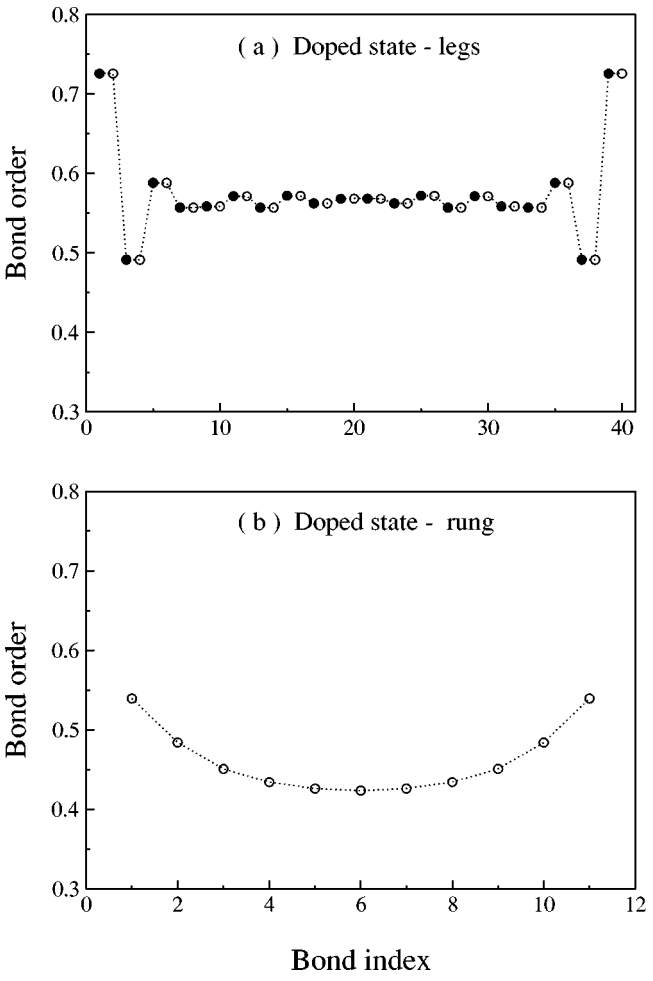

FIG. 14. Bond order in the singly doped state for polyacene, (a) for the legs of the ladder, (b) for the rungs. In (a) the filled circles represent the top leg and the empty circles the bottom leg of the ladder. The numbering scheme for the bonds again follows that in Fig. 2.

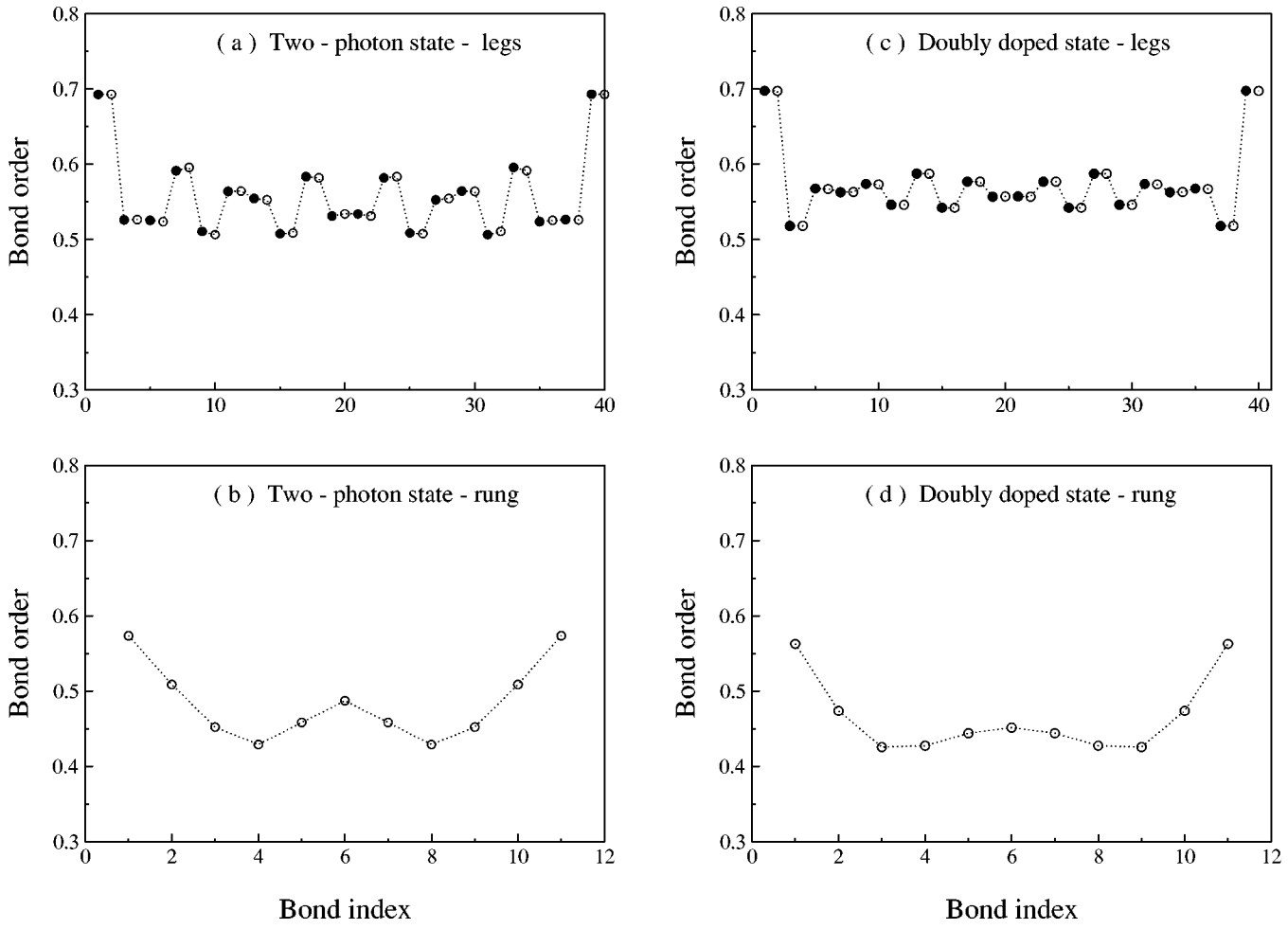

FIG. 15. Bond order in the 2^1A^+ and negative bipolaron states for polyacene, (a) for bonds on the legs, (b) for bonds on the rung for 2^1A^+ state, (c) for bonds on the legs, and (d) for bonds on the rung for negative bipolaron state. The empty circles represent the top leg and the filled circles the bottom leg of the ladder in (a) and (c). The bond index corresponds to the numbering scheme in Fig. 2.

The state can be thought of as consisting of two triplets. It appears from the rung bond analysis of the two-photon state that indeed two minima are found in the rung bond length as against one minima in the triplet state. However, energetically such a relation does not seem to exist.

IV. SUMMARY

We have studied the nature of the excited states of polyacene with up to ten rings, using the symmetrized DMRG method, taking into account long-range Coulomb interactions within a PPP model. We find that the symmetrized DMRG method is quite accurate for the polyacenes even in the presence of long-range interactions. In the long chain limit, we find that the two-photon state lies below the lowest dipole allowed one-photon state. The triplet gap is much smaller than half the two-photon gap showing that the two-photon state in polyacenes is qualitatively different from those in the linear polyenes. In short oligomers, the two-photon state lies above the one-photon state. In the polymer limit the triplet gap is 0.53 eV, the two-photon gap is 1.71 eV, and the optical gap is 2.46 eV. These results are in agreement with the general trends observed in conjugated polymers. We have calculated the charge excitation gap and the optical gap for the system and have estimated the binding energy of the 1^1B^- exciton to be 2.09 eV. We have also studied singly and doubly doped systems. The bipolaron is found to consist of two separate polarons. From bond orders we find that the ground state in relaxed geometry would have equal bond lengths along the legs, with the rung bonds being longer than the leg bonds. In the triplet state, the dipole allowed state, and the polarons, the chain bonds show an alternation in bond length while the rung bonds tend to be longer in the middle of the system. The bond order pattern in the two-photon state shows that the state is more delocalized than the other excited states we have considered.

ACKNOWLEDGMENTS

This work has been supported by grants from the Council for Scientific and Industrial Research (CSIR), India, and by the Board for Research in Nuclear Sciences (BRNS), India.

*Email address: raghu@sscu.iisc.ernet.in
†Email address: anusooya@sscu.iisc.ernet.in
‡Email address: ramasesh@sscu.iisc.ernet.in

[1] J. Schön, Ch. Kloc, A. Dodabalapur, and B. Batlogg, Science **289**, 599 (2000).
[2] J.H. Schön, Ch. Kloc, and B. Batlogg, Science **288**, 2338 (2000).
[3] J.H. Schön, Ch. Kloc, and B. Batlogg, Nature (London) **406**, 702 (2000).
[4] J.H. Schön, S. Berg, Ch. Kloc, and B. Batlogg, Science **287**, 1022 (2000).
[5] A. Shukla and S. Mazumdar, Phys. Rev. Lett. **83**, 3944 (1999).
[6] H.C. Longuet-Higgins and L. Salem, Proc. R. Soc. London, Ser. A **251**, 172 (1959); **255**, 435 (1960).
[7] C. Raghu, Y. Anusooya Pati, and S. Ramasesha, Phys. Rev. B **65**, 155204 (2002).
[8] T. Hashimoto, H. Nakano, and K. Hirao, J. Chem. Phys. **104**, 6244 (1996).
[9] J. Cornil, J.Ph. Calbert, and J.L. Bredas, J. Am. Chem. Soc. **123**, 1250 (2001).
[10] H. Naarmann, (unpublished).
[11] W.P. Su, J.R. Schrieffer, and A.J. Heeger, Phys. Rev. B **22**, 2099 (1980).
[12] D. Baeriswyl and K. Maki, Phys. Rev. B **28**, 2068 (1983).
[13] M.K. Sabra, Phys. Rev. B **53**, 1269 (1996).
[14] Z.J. Li, H.Q. Lin, and K.L. Yao, Z. Phys. B: Condens. Matter **104**, 77 (1997).
[15] Z.G. Soos, S. Ramasesha, and D.S. Galvao, Phys. Rev. Lett. **71**, 1609 (1993).
[16] Z.G. Soos and S. Ramasesha, Phys. Rev. B **29**, 5410 (1984).
[17] P. Tavan and K. Schulten, J. Chem. Phys. **85**, 6602 (1986).
[18] P. Tavan and K. Schulten, Phys. Rev. B **36**, 4337 (1987).
[19] R. Pariser and R.G. Parr, J. Chem. Phys. **21**, 446 (1953); J.A. Pople, Trans. Faraday Soc. **49**, 1375 (1953).
[20] For a review, see S. Mazumdar, *Conjugated Conducting Polymers*, edited by H. G. Kiess (Springer-Verlag, Berlin, 1992), pp. 7-134.
[21] S. Ramasesha, G.S. Galvao, and Z.G. Soos, J. Phys. Chem. **97**, 2823 (1993).
[22] For a review, see *Density-Matrix Renormalization: A New Numerical Method in Physics*, Lecture Notes in Physics Vol. 528, edited by I. Peschel, X. Wang, M. Kaulke, and K. Hallberg (Springer, New York, 1999), pp. 247-260.
[23] S. Ramasesha, Swapan K. Pati, H.R. Krishnamurthy, Z. Shuai, and J.L. Bredas, Phys. Rev. B **54**, 7598 (1996).
[24] K. Ohno, Theor. Chim. Acta **2**, 219 (1964).
[25] S.R. White Phys. Rev. Lett. **69**, 2863 (1992); , Phys. Rev. B **48**, 10 345 (1992).
[26] Z. G. Soos and S. Ramasesha in *Valence Bond Theory and Chemical Structure*, edited by D. J. Klein and N. Trinajstić (Elsevier, New York, 1990).
[27] Z. Shuai, S.K. Pati, W.P. Su, J.L. Bredas, and S. Ramasesha, Phys. Rev. B **56**, 9298 (1997).
[28] Z.G. Soos, S. Ramasesha, and D.S. Galvao, Phys. Rev. Lett. **71**, 1609 (1993).
[29] Y. Kawashima, T. Hashimoto, H. Nakano, and K. Hirao, Theor. Chem. Acc. **102**, 49 (1999).
[30] Z. Shuai, S.K. Pati, W.P. Su, J.L. Bredas, and S. Ramasesha, Phys. Rev. B **55**, 15 368 (1997).
[31] C.A. Coulson, Proc. R. Soc. London, Ser. A **164**, 383 (1938).
[32] H.B. Klevens and J.R. Platt, J. Chem. Phys. **17**, 470 (1949).
[33] J. Schiedt and R. Weinkauf, Chem. Phys. Lett. **266**, 201 (1997).
[34] N. Sato, H. Inokuchi, and E.A. Silinsh, Chem. Phys. **115**, 269 (1987).
[35] N. Sabbatini, M.T. Indelli, M.T. Gandolfi, and V. Balzani, J. Phys. Chem. **86**, 3585 (1982).
[36] T.M. Halasinski, D.M. Hudgins, F. Salama, L.J. Allamandola, and T. Bally, J. Phys. Chem. A **104**, 7484 (2000).